# Association of GLOD4 with Alzheimer's Disease in Humans and Mice

Olga Utyro [a, #], Olga Włoczkowska-Łapińska [a, #], Hieronim Jakubowski [a,b,*]

[a] *Department of Biochemistry and Biotechnology, Poznań University of Life Sciences, Poznań, Poland*

[b] *Department of Microbiology, Biochemistry & Molecular Genetics, Rutgers-New Jersey Medical School, International Center for Public Health, 225 Warren Street, Newark, NJ, USA*

[#]These authors contributed equally to this work.

*Correspondence to: Hieronim Jakubowski, Department of Microbiology, Biochemistry and Molecular Genetics, Rutgers-New Jersey Medical School, International Center for Public Health, 225 Warren Street, Newark, New Jersey 07103, USA; E-mail: jakubows@rutgers.edu

## Abstract

Glyoxylase domain containing protein (GLOD4) is associated with Alzheimer's disease (AD). We quantified GLOD4 in human AD brains, mouse AD model, and neuroblastoma N2a-APPswe cells. We found that GLOD4 was downregulated in human AD patients compared to non-AD controls. Glod4 was similarly downregulated in *Blmh*$^{-/-}$5xFAD mouse model of AD. Downregulated Glod4 was associated with elevated Aβ and worsened memory/sensorimotor performance in *Blmh*$^{-/-}$5xFAD mice. Glod4 depletion in N2a-APPswe cells upregulated AβPP and downregulated autophagy-related Atg5 and p62 genes. These findings suggest that Glod4 interacts with AβPP and the autophagy pathway, disruption of these interactions leads to Aβ accumulation and cognitive/neurosensory deficits.

**Keywords:** GLOD4, Alzheimer's disease; APP; Bleomycin hydrolase; *Blmh*$^{-/-}$*5xFAD* mouse; N2a-APPswe mouse neuroblastoma cells; Atg5; p62; autophagy

## INTRODUCTION

The glyoxalase domain containing protein 4 (GLOD4) is encoded by the *GLOD4* gene (C17orf25) found in a region on human chromosome 17 showing high heterozygosity in human hepatocellular carcinoma [1]. Human GLOD4 is expressed in most tissues, including the brain [1] (https://www.proteinatlas.org/ENSG00000167699-GLOD4). GLOD4 belongs to the glycosylate gene family that includes glycosylase 1 (GLO1), which detoxifies methylglyoxal [2].

Methylglyoxal, a byproduct of glucose metabolism [3] responsible for protein glycation can causes misfolding [4]. Glycosylated proteins easily aggregate, which can give rise to amyloid plaques, a hallmark of Alzheimer's disease (AD) [5]. Although human GLOD4 was suggested to take part in the methylglyoxal detoxification [6], this still is to be shown.

The human GLOD4 protein has 3 isoforms, differing in amino acid sequence (www.uniprot.org/blast/). The isoform 1 consists of 313 amino acids and contains motifs of the glyoxalase domain [2], antibiotic resistance domain, and a domain characteristic of the family of proteins resistant to the cytotoxic anticancer drug bleomycin (www.ncbi.nlm.nih.gov/protein/NP_057164.3). A yeast two-hybrid screen showed that GLOD4 protein interacts with mitochondrial ADP-ribose pyrophosphatase NUDT9, which may regulate cell growth [7].

There is some evidence suggesting that GLOD4 may play an important role on the central nervous system (CNS) and may be linked to AD. For instance, the *GLOD4* rs2750012 polymorphism was associated with AD in the Arab population of northern Israel. This association has been replicated in metanalysis performed in seven independent GWAS datasets [8]. Levels of Glod4 protein isoform 3 were significantly elevated in APPSwDI/*NOS2*$^{-/-}$ mouse model of AD compared with controls [6]. Proteomic studies of microglial cells BV-2 showed that treatments with the anti-inflammatory drug polyphenol pentagalloyl glucose attenuated GLOD4 protein level while treatments with proinflammatory LPS/IFNγ elevated GLOD4. *GLOD4* was among 38 duplicated genes multiple cases of autism spectrum disorder (ASD) [9].

Bleomycin hydrolase (BLMH) plays a key role in the CNS and is linked to AD. For example, BLMH can process amyloid precursor protein (AβPP) to amyloid β (Aβ) [10] and to further process Aβ[11]. Enzymatic activities of BLMH are significantly downregulated in the human AD brain [12]. *Blmh*$^{-/-}$ mice show astrogliosis, behavioral changes [13], *and* diminished ability to detoxify Hcy-thiolactone, which elevates brain Hcy-thiolactone level and increases its neurotoxicity [4]. Proteomic studies of *Blmh*$^{-/-}$

mouse brain show that Blmh interacts with diverse cellular processes, such as synaptic plasticity, cytoskeleton dynamics, cell cycle, energy metabolism, and antioxidant defenses that are essential for brain homeostasis [9]. *Blmh*$^{-/-}$5xFAD mouse model of AD shows exacerbated cognitive/neuromotor deficits [14]. These neurological impairments resulted from the disruption of interactions of Blmh with AβPP and the Phf8/H4K20me1/mTOR/autophagy pathway, which lead to Aβ accumulation and cognitive/neuromotor deficits [14].

Here we examined the role of GLOD4 in the CNS by studying GLOD4 expression in AD brains. We also examined Glod4 expression in *Blmh*$^{-/-}$5xFAD mouse model of AD in relation to cognitive/neuromotor performance in these mice and biochemical consequences of *Glod4* gene silencing in mouse neuroblastoma N2a-APPswe cells. Our findings show that GLOD4 is important for CNS homeostasis.

## MATERIALS AND METHODS

### *Human brain samples*

Human brain cerebral cortical tissues were obtained at autopsy by the Case Western Reserve University Brain Bank under an IRB-approved protocol, from clinically and pathologically confirmed cases of AD (n = 6) using criteria set up by the National Institute of Aging (NIA) and Consortium to Establish a Registry for Alzheimer's Disease (CERAD) [15]. Brain tissues were also obtained from non-AD control patients (n = 6). Samples of frontal cortex, coded prior to shipment to keep laboratory personnel blinded as to diagnosis, were shipped on dry ice to the New Jersey Medical School and stored at−80◦C until used. The AD patients were 84±8-year-old, 67% female, post-mortem interval was 8±5 h. Controls were 77±6-year-old ($P$ = 0.100), 83% female ($P$ = 0.549), post-mortem interval was 16±8 ($P$ = 0.103).

### *Mice*

*Blmh*$^{-/-}$5xFAD and *Blmh*$^{+/+}$5xFAD mice, obtained by crossing *Blmh*$^{-/-}$ and 5xFAD animals, were characterized in an earlier study [14]. *Blmh* [16] and 5xFAD [17] genotypes were established by PCR using primers listed in **Table 1**. Mice were kept at the Rutgers-New Jersey Medical School Animal Facility as previously described [14]. Five-month-old were used in experiments. Animal procedures were approved by the Institutional Animal Care and Use Committee at Rutgers-New Jersey Medical School.

### *Behavioral testing*

Cognitive and neuromotor performance was evaluated using the novel object recognition [18] and the hindlimb [19] tests as previously described [14].

*Brain protein extraction*

Human and mouse brain proteins were extracted as previously described [14].

*Cell culture and Glod4 siRNA transfection*

Mouse neuroblastoma N2a-APPswe cells, harboring a human AβPP transgene with the K670N and M671L Swedish mutations associated with familial early-onset AD [20] were grown (37°C, 5% $CO_2$) in DMEM/F12 medium (Thermo Scientific) supplemented with 5% FBS, non-essential amino acids, and antibiotics (penicillin/streptomycin) (MilliporeSigma).

Cell monolayers (70-80% confluency), washed twice with PBS, were transfected with *Glod4*-targeting siRNAs (siRNA Glod4 #1: Cat. #43390816 ID s84641; siRNA Glod4 #1: Cat. #4390816 ID s84642) (Thermo Scientific) in Opti-MEM medium with Lipofectamine RNAiMax (Thermo Scientific) for 24 hours.

*Western blots*

Proteins were extracted using RIPA buffer (MilliporeSigma), separated by SDS-PAGE, and quantified with the following antibodies: anti-GLOD4 (Aviva Systems Biology, OAGA00314), anti-GAPDH (MilliporeSigma PLA0125), anti-Glod4 (Abcam, AB188371), anti-App (Abcam, ab126732), anti-βactin (Abcam ab8227), anti-Phf8 (Abcam, ab36068), anti-mTOR (CS #2983), anti-Atg5 (CS, #12994), anti-Atg7 (CS, #8558), anti-Becn1 (CS, #3495), or anti-Gapdh (CS, #5174) for 1 hour. Membranes were washed three times with TBST, 10 min each, and incubated with goat anti-rabbit IgG secondary antibody conjugated with horseradish peroxidase. Positive signals were detected using Western Bright Quantum-Advansta K12042-D20 and GeneGnome XRQ NPC chemiluminescence detection system. Bands intensity was calculated using Gene Tools program from Syngene.

*RNA isolation, cDNA synthesis, RT-qPCR analysis*

Total RNA was isolated using Trizol reagent (MilliporeSigma). cDNA was synthesized using Revert Aid First cDNA Synthesis Kit (Thermo Fisher Scientific) according to manufacturer's protocol. Nucleic acid concentration was measured using NanoDrop (Thermo Fisher Scientific). RT-qPCR was performed with SYBR Green Mix and CFX96 thermocycler (Bio-Rad). The $2^{(-\Delta\Delta Ct)}$ method was used to calculate the relative expression levels [21]. Data were analyzed using CFX Manager™ Software and Microsoft Excel. RT-qPCR primer sequences are listed in **Table 1**.

*Data analysis*

Normality of distributions was tested with the Shapiro-Wilk's statistic. For variables with normal distributions, The results were calculated as mean±SD for variables with normal distributions or medians for non-normally distributed variables. A parametric unpaired t test was used for comparisons between two groups of variables with normal distribution. A Mann-Whitney rank sum test was used for comparisons between two groups of non-normally distributed variables.

**RESULTS**

*GLOD4 is downregulated in AD brains*

Three isoforms of GLOD4 exist in humans: 34.8 kDa isoform 1 (GLOD4_1), 33.2 kDa isoform 2 (GLOD4_2), and 21.3 kDa isoform 3 (GLOD4_3). We quantified mRNA encoding these isoforms in brains of AD patients and controls by using RT-qPCR.

We found that GLOD4_1 mRNA level was the highest in control human brains; GLOD4_2 and GLOD4_3 mRNAs were present at 10-fold lower levels (**Figure 1A**). Similar pattern of GLOD4 isoforms expression was seen in AD brains (**Figure 1A**). However, relative levels of GLOD4 mRNA isoforms were significantly reduced in AD brains: from 10.31 to 3.83 (by 63%) for GLOD4_1 mRNA, from 1.00 to 0.51 (by 49%) for GLOD4_2 mRNA, and from 1.10 to 0.30 (by 73%) for GLOD4_3 mRNA (**Figure 1A**).

GLOD4 protein, quantified by western blotting, was similarly downregulated in human AD brains. SDS-PAGE analyses revealed two bands reacting with anti-GLOD4 antibody in brain protein extracts: an upper band of 35/33 kDa likely corresponding to GLOD4_1 and GLOD4_2 and a lower band of 21 kDa likely corresponding to GLOD4_3, based on the molecular weight (**Figure 1C**). Quantification showed that GLOD4_1/2 protein level was significantly reduced in AD brains compared to controls (0.62 vs. 1.00) as was the level of GLOD4_3 protein (0.63 vs. 1.00) (**Figure 1B**).

*Glod4 level is associated with Aβ and cognitive/neuromotor performance in Blmh$^{-/-}$5xFAD mice*

To determine whether downregulated GLOD4 level seen in AD patients are associated with hallmarks of AD, we quantified Glod4 level in *Blmh*$^{-/-}$5xFAD mice, a model of human AD; *Blmh*$^{+/+}$5xFAD littermates were used as controls [14]. Earlier work has shown that Glod4_1 is a major isoform while Glod4_3 is a minor isoform in mice. We found that Glod4_1 mRNA was significantly downregulated in *Blmh*$^{-/-}$5xFAD brains compared to *Blmh*$^{+/+}$5xFAD sibling controls (**Figure 2A**), thus recapitulating the findings in the human AD brain (**Figure 1A**). Low Glod4 expression level in *Blmh*$^{-/-}$5xFAD brains was accompanied by elevated Aβ level (**Figure 2B**).

Behavioral testing showed that *Blmh*$^{-/-}$5xFAD mice with lower Glod4 level also had neurological impairments characteristic of human AD. Specifically, these mice did not differentiate between novel

and familiar objects in the NOR test, which shows impaired recognition memory. In contrast, *Blmh*$^{+/+}$5xFAD mice that had higher Glod4_1 level also had normal preference for novelty (**Figure 2C**).

In the hindlimb clasping test, *Blmh*$^{-/-}$5xFAD mice that showed downregulated Glod4_1 level also showed significantly higher scores (indicating neuromotor deficits) compared to *Blmh*$^{+/+}$5xFAD animals that had higher Glod4_1 (**Figure 1A**) and lower scores (i.e., better neuromotor performance) **(Figure 2D**).

*Glod4 silencing affects APP and autophagy related Atg5 and p62 mRNAs in mouse cells*

To elucidate the mechanism by which Glod4 can affect behavioral hallmarks of AD, we first examined whether our findings of downregulated GLOD4 in AD patients (**Figure 1A**) can be recapitulated in mouse neuroblastoma cells N2a-APPswe carrying a mutated human AβPP transgene. We silenced the *Glod4* gene by RNA interference using siRNA Glod4#1 and siRNA Glod4#2 for transfections; controls were transfected with scrambled siRNA (siRNAscr). Gene expression was examined by RT-qPCR using β-actin mRNA as a reference.

We found that the Glod4_1 mRNA level was significantly reduced in *Glod4*-silenced cells (by 76% for siRNA Glod4#1 and 98% for siRNA Glod4#2; **Figure 3A**). Glod4 protein was similarly downregulated in the silenced cells (**Figure 3B**). The downregulation of Glod4 expression was accompanied by upregulation of AβPP expression (**Figure 3C, D**). At the same time, autophagy mRNAs for Atg5 (the regulator of autophagosome assembly) (**Figure 3E**) and p62 (a receptor for degradation of ubiquitinated substrates) (**Figure 3F**) were significantly downregulated.

To find whether the effects of Glod4 silencing on autophagy could be mediated by mTOR signaling, we quantified levels of PHF8 (a positive regulator of mTOR expression) in *Glod4*-silenced and control cells. We found that Phf8 and mTOR was not affected by the *Glod4* gene silencing (not shown).

**DISCUSSION**

Our findings suggest that Glod4, a protein with an unknown function, has a protective role in the CNS. Specifically, we showed that (*i*) GLOD4 was downregulated in human AD patients compared to non-AD controls; (*ii*) Glod4 was similarly downregulated in *Blmh*$^{-/-}$5xFAD mouse AD model; (*iii*) downregulated Glod4 level was associated with worsened memory/sensorimotor performance in *Blmh*$^{-/-}$ 5xFAD mice (*iv*); Glod4 depletion in N2a-APPswe cells upregulated AβPP and downregulated autophagy-related Atg5 and p62 genes). These findings suggest that Aβ accumulation in Glod4-depleted brains can occur via two pathways shown in Fig. 4.

In the first pathway, GLOD4 depletion upregulates AβPP, which will increase the accumulation of Aβ leading to cognitive/neuromotor impairments. In the second pathway, GLOD4 depletion downregulates Atg5 and p62, which will impair autophagy and thus increase Aβ and cognitive/neuromotor impairments. That impaired autophagy can increase Aβ accumulation mediated by AβPP is known. For example, Becn1, a protein initiating autophagy, is decreased in human AD brains while genetic reduction of Becn1 in transgenic mice that overexpress AβPP (*APP*$^{+}$*Becn*$^{+/-}$ mice) increased Aβ in neuronal cells [22]. However, as we did not find any effect of Glod4 depletion on Becn1 expression (not shown), Glod4 depletion upregulates APP by a Becn1-independent mechanism.

We found that major GLOD4_1 isoform, and minor GLOD4_2 and GLOD4_3 isoforms, were expressed in human brain. All three isoforms were similarly attenuated in AD brains, suggesting that GLOD4 isoforms are unlikely to have an isoform-specific function in AD.

In conclusion, our findings suggest that Glod4 interacts with AβPP and the autophagy pathway, and that disruption of these interactions upregulates Aβ, which causes cognitive/neurosensory deficits, thereby highlighting Glod4 role in brain homeostasis. Further studies are needed to assess causality of the association of GLOD4 depletion with AD.

**ACKNOWLEDGMENTS**

We thank H.G. Lee for samples of AD and control human brains, S.S. Sisodia for the mouse neuroblastoma N2a-APPswe cells and J. Lazo for the Blmh$^{-/-}$ mouse.

**FUNDING**

Supported in part by grants 2015/17/N/NZ3/03626, 2018/29/B/NZ4/00771, 2019/33/B/NZ4/01760, and 2021/43/B/NZ4/00339 from the National Science Center, Poland, and Grant 17GRNT32910002 from the American Heart Association.

**CONFLICT OF INTEREST**

Hieronim Jakubowski is an Editorial Board Member of this journal but was not involved in the peer-review process nor had access to any information about its peer-review. All other authors have no conflict of interest to report.

**DATA AVAILABILITY**

The data that support the findings of this study are available in the methods and/or supplementary material of this article.

**REFERENCES**


[1] Qin WX, Wan F, Sun FY, Zhang PP, Han LW, Huang Y, Jiang HQ, Zhao XT, He M, Ye Y, Cong WM, Wu MC, Zhang LS, Yang NW, Gu JR (2001) Cloning and characterization of a novel gene (C17orf25) from the deletion region on chromosome 17p13.3 in hepatocelular carcinoma. *Cell Res* **11**, 209-216.

[2] Farrera DO, Galligan JJ (2022) The Human Glyoxalase Gene Family in Health and Disease. *Chem Res Toxicol* **35**, 1766-1776.

[3] Thornalley PJ (1996) Pharmacology of methylglyoxal: formation, modification of proteins and nucleic acids, and enzymatic detoxification--a role in pathogenesis and antiproliferative chemotherapy. *Gen Pharmacol* **27**, 565-573.

[4] Li XH, Xie JZ, Jiang X, Lv BL, Cheng XS, Du LL, Zhang JY, Wang JZ, Zhou XW (2012) Methylglyoxal induces tau hyperphosphorylation via promoting AGEs formation. *Neuromolecular Med* **14**, 338-348.

[5] Gomes R, Sousa Silva M, Quintas A, Cordeiro C, Freire A, Pereira P, Martins A, Monteiro E, Barroso E, Ponces Freire A (2005) Argpyrimidine, a methylglyoxal-derived advanced glycation end-product in familial amyloidotic polyneuropathy. *Biochem J* **385**, 339-345.

[6] Hoos MD, Richardson BM, Foster MW, Everhart A, Thompson JW, Moseley MA, Colton CA (2013) Longitudinal study of differential protein expression in an Alzheimer's mouse model lacking inducible nitric oxide synthase. *J Proteome Res* **12**, 4462-4477.

[7] Zhang HT, Yan ZQ, Hu XB, Yang SL, Gong Y (2003) Interaction of C17orf25 with ADP-ribose pyrophosphatase NUDT9 detected via yeast two-hybrid method. *Sheng Wu Hua Xue Yu Sheng Wu Wu Li Xue Bao (Shanghai)* **35**, 747-751.

[8] Sherva R, Baldwin CT, Inzelberg R, Vardarajan B, Cupples LA, Lunetta K, Bowirrat A, Naj A, Pericak-Vance M, Friedland RP, Farrer LA (2011) Identification of novel candidate genes for Alzheimer's disease by autozygosity mapping using genome wide SNP data. *J Alzheimers Dis* **23**, 349-359.

[9] Zarrei M, Burton CL, Engchuan W, Young EJ, Higginbotham EJ, MacDonald JR, Trost B, Chan AJS, Walker S, Lamoureux S, Heung T, Mojarad BA, Kellam B, Paton T, Faheem M, Miron K, Lu C, Wang T, Samler K, Wang X, Costain G, Hoang N, Pellecchia G, Wei J, Patel RV, Thiruvahindrapuram B, Roifman M, Merico D, Goodale T, Drmic I, Speevak M, Howe JL, Yuen RKC, Buchanan JA, Vorstman JAS, Marshall CR, Wintle RF, Rosenberg DR, Hanna GL, Woodbury-Smith M, Cytrynbaum C, Zwaigenbaum L, Elsabbagh M, Flanagan J, Fernandez BA, Carter MT, Szatmari P, Roberts W, Lerch J, Liu X, Nicolson R, Georgiades S, Weksberg R, Arnold PD, Bassett AS, Crosbie J, Schachar R, Stavropoulos DJ, Anagnostou E, Scherer SW (2019) A large data resource of genomic copy number variation across neurodevelopmental disorders. *NPJ Genom Med* **4**, 26.

[10] Lefterov IM, Koldamova RP, Lazo JS (2000) Human bleomycin hydrolase regulates the secretion of amyloid precursor protein. *Faseb J* **14**, 1837-1847.

[11] Kajiya A, Kaji H, Isobe T, Takeda A (2006) Processing of amyloid beta-peptides by neutral cysteine protease bleomycin hydrolase. *Protein Pept Lett* **13**, 119-123.

[12] Suszynska J, Tisonczyk J, Lee HG, Smith MA, Jakubowski H (2010) Reduced homocysteine-thiolactonase activity in Alzheimer's disease. *J Alzheimers Dis* **19**, 1177-1183.

[13] Towne CF, York IA, Watkin LB, Lazo JS, Rock KL (2007) Analysis of the role of bleomycin hydrolase in antigen presentation and the generation of CD8 T cell responses. *J Immunol* **178**, 6923-6930.

[14] Witucki L, Borowczyk K, Suszynska-Zajczyk J, Warzych E, Pawlak P, Jakubowski H (2023) Deletion of the Homocysteine Thiolactone Detoxifying Enzyme Bleomycin Hydrolase, in Mice, Causes Memory and Neurological Deficits and Worsens Alzheimer's Disease-Related Behavioral and Biochemical Traits in the 5xFAD Model of Alzheimer's Disease. *J Alzheimers Dis*.

[15] Khachaturian ZS (1985) Diagnosis of Alzheimer's disease. *Arch Neurol* **42**, 1097-1105.

[16] Schwartz DR, Homanics GE, Hoyt DG, Klein E, Abernethy J, Lazo JS (1999) The neutral cysteine protease bleomycin hydrolase is essential for epidermal integrity and bleomycin resistance. *Proc Natl Acad Sci U S A* **96**, 4680-4685.

[17] Oakley H, Cole SL, Logan S, Maus E, Shao P, Craft J, Guillozet-Bongaarts A, Ohno M, Disterhoft J, Van Eldik L, Berry R, Vassar R (2006) Intraneuronal beta-amyloid aggregates, neurodegeneration, and neuron loss in transgenic mice with five familial Alzheimer's disease mutations: potential factors in amyloid plaque formation. *J Neurosci* **26**, 10129-10140.

[18] Leger M, Quiedeville A, Bouet V, Haelewyn B, Boulouard M, Schumann-Bard P, Freret T (2013) Object recognition test in mice. *Nat Protoc* **8**, 2531-2537.

[19] Lieu CA, Chinta SJ, Rane A, Andersen JK (2013) Age-related behavioral phenotype of an astrocytic monoamine oxidase-B transgenic mouse model of Parkinson's disease. *PLoS One* **8**, e54200.

[20] Thinakaran G, Teplow DB, Siman R, Greenberg B, Sisodia SS (1996) Metabolism of the "Swedish" amyloid precursor protein variant in neuro2a (N2a) cells. Evidence that cleavage at the "beta-secretase" site occurs in the golgi apparatus. *J Biol Chem* **271**, 9390-9397.

[21] Livak KJ, Schmittgen TD (2001) Analysis of relative gene expression data using real-time quantitative PCR and the 2(-Delta Delta C(T)) Method. *Methods* **25**, 402-408.

[22] Pickford F, Masliah E, Britschgi M, Lucin K, Narasimhan R, Jaeger PA, Small S, Spencer B, Rockenstein E, Levine B, Wyss-Coray T (2008) The autophagy-related protein beclin 1 shows reduced expression in early Alzheimer disease and regulates amyloid beta accumulation in mice. *J Clin Invest* **118**, 2190-2199.

**Figure legends**

**Figure 1.** Reduced expression of GLOD4 in brains of Alzheimer's disease patients. Isoforms of GLOD4 mRNA (A) and protein (B) were quantified by RT-qPCR and western blotting, respectively. Representative image of western blot is shown in panel (C).

**Figure 2.** Reduced level of brain Glod 4 is associated with elevated amyloid β and impaired cognitive/neuromotor performance in a mouse model of Alzheimer's disease. Five-month-old *Blmh*$^{-/-}$ 5xFAD mice (n = 22) and their *Blmh*$^{+/+}$5XFAD siblings (n = 15) were used in the experiments. Bar graphs illustrate quantification of Glod4 mRNA (A), amyloid β (B), and cognitive/neuromotor performance in the NOR (C) and hindlimb (D) tests. β-Actin mRNA was used as a reference for normalization in (A). Panels B, C, and D were reproduced with permission from [14]. Data points for each mouse group represent mean ± SD of two to four independent measurements for each mouse.

**Figure 3.** *Glod4* gene silencing affects expression of AβPP and autophagy-related proteins in mouse neuroblastoma N2a-APPswe cells. N2a-APPswe cells were transfected with two different siRNAs targeting the *Glod4* gene (siRNA Glod4 #1 and siRNA Glod4 #2) or scrambled siRNA (siRNAscr) as a control. Proteins and mRNAs were quantified by western blotting and RT-qPCR. Bar graphs illustrate quantification of (A) Glod4, (C) AβPP, (E) Atg5, and (F) p62 mRNAs; and Glod4 (B) and AβPP proteins (D). Insets is (B) and (D) show representative western blots for Glod4 and AβPP, respectively in control and siRNA Glod4-sileneced cells. Each data point is an average ± SD of three replicate measurements for three independent biological replicates. Panel (G) illustrates hypothetical pathways by which GLOD4 depletion can contribute to Aβ accumulation and neurological impairments in AD.

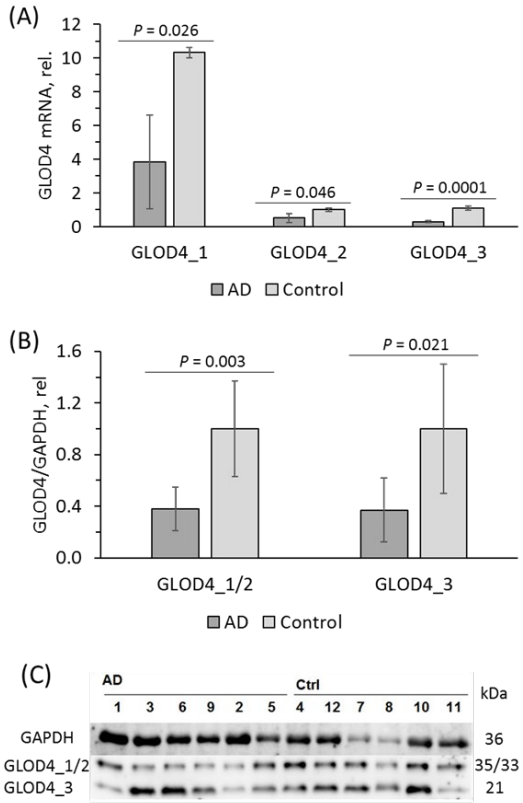
(A)
GLOD4 mRNA, rel.
12
10
8
6
4
2
0
P = 0.026
P = 0.046
P = 0.0001
GLOD4_1
GLOD4_2
GLOD4_3
AD
Control
(B)
GLOD4/GAPDH, rel
1.6
1.2
0.8
0.4
0.0
P = 0.003
P = 0.021
GLOD4_1/2
GLOD4_3
AD
Control
(C)
AD
Ctrl
1 3 6 9 2 5 4 12 7 8 10 11
kDa
GAPDH
GLOD4_1/2
GLOD4_3
36
35/33
21

Figure 1

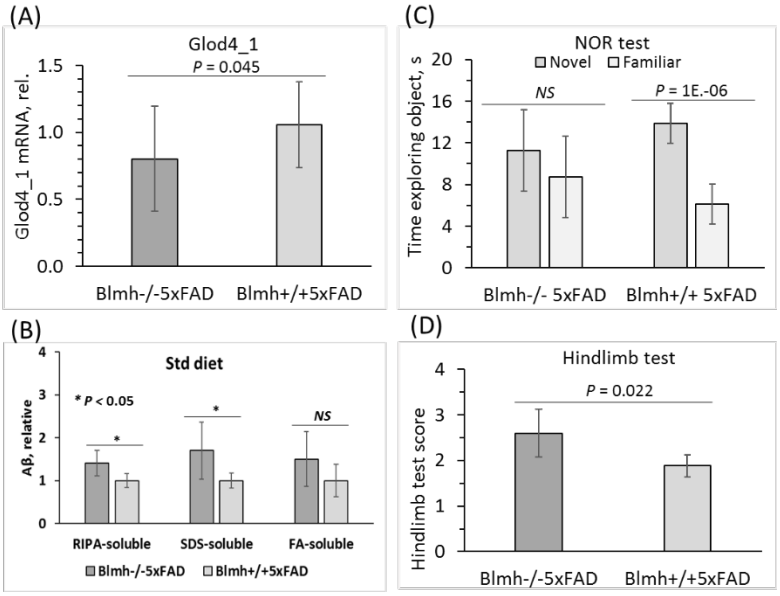
(A)
Glod4_1
P = 0.045
Glod4_1 mRNA, rel.
1.5
1.0
0.5
0.0
Blmh-/-5xFAD
Blmh+/+5xFAD
(C)
NOR test
Novel
Familiar
NS
P = 1E.-06
Time exploring object, s
20
16
12
8
4
0
Blmh-/- 5xFAD
Blmh+/+ 5xFAD
(B)
Std diet
* P < 0.05
*
*
NS
Aβ, relative
4
3
2
1
0
RIPA-soluble
SDS-soluble
FA-soluble
Blmh-/-5xFAD
Blmh+/+5xFAD
(D)
Hindlimb test
P = 0.022
Hindlimb test score
4
3
2
1
0
Blmh-/-5xFAD
Blmh+/+5xFAD

Figure 2

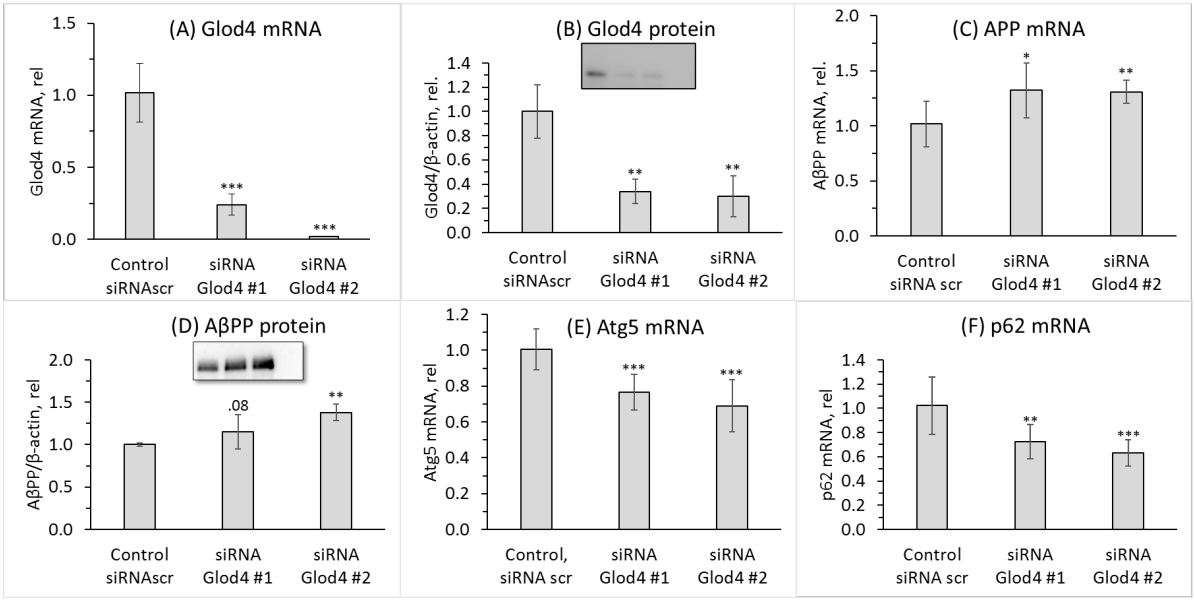
(A) Glod4 mRNA
Glod4 mRNA, rel
1.5
1.0
0.5
0.0
***
***
Control siRNAscr
siRNA Glod4 #1
siRNA Glod4 #2
(B) Glod4 protein
Glod4/β-actin, rel.
1.4
1.2
1.0
0.8
0.6
0.4
0.2
0.0
**
**
Control siRNAscr
siRNA Glod4 #1
siRNA Glod4 #2
(C) APP mRNA
AβPP mRNA, rel.
2.0
1.5
1.0
0.5
0.0
*
**
Control siRNA scr
siRNA Glod4 #1
siRNA Glod4 #2
(D) AβPP protein
AβPP/β-actin, rel
2.0
1.5
1.0
0.5
0.0
.08
**
Control siRNAscr
siRNA Glod4 #1
siRNA Glod4 #2
(E) Atg5 mRNA
Atg5 mRNA, rel
1.2
1.0
0.8
0.6
0.4
0.2
0.0
***
***
Control, siRNA scr
siRNA Glod4 #1
siRNA Glod4 #2
(F) p62 mRNA
p62 mRNA, rel
1.4
1.2
1.0
0.8
0.6
0.4
0.2
0.0
**
***
Control siRNA scr
siRNA Glod4 #1
siRNA Glod4 #2

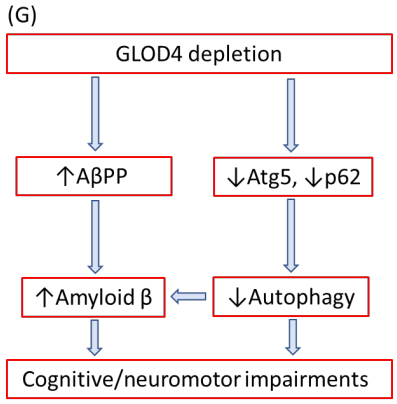
(G)
GLOD4 depletion
↑AβPP
↓Atg5, ↓p62
↑Amyloid β
↓Autophagy
Cognitive/neuromotor impairments

Figure 3

**Supplementary Material**

| **Table S1** Primers used for PCR or RT-qPCR | |
|---|---|
| *Gene* | *Primer sequence* |
| *GLOD4 isoform 1* | *Forward: 5'-CACCCGGATAACAGAAGACAGTT-3'* |
| | *Reverse: 5'-TTCCAAAAGCTGCTGCATG-3'* |
| *GLOD4 isoform 2* | *Forward: 5'-CACCCGGATAACAGAAGACAGTT-3'* |
| | *Reverse: 5'-CTTGTAGTCTCCGACGCCAT-3'* |
| *GLOD4 isoform 3* | *Forward: 5'-GCAGTGTCTGATCTTCAAAAGTCC-3'* |
| | *Reverse: 5'-TTCTCCAAGATTGCTCACCTGG-3'* |
| *B2M* | *Forward: 5'-GGGTTTCATCCATCCGACA-3'* |
| | *Reverse: 5'- ACACGGCAGGCATACTCATC -3'* |
| *Glod4 isoform 1* | *Forward: 5'-CTTGCTTCTAGCCAAGCTGT-3'* |
| | *Reverse: 5'-AGACACTGCTAGAGTCACCT-3'* |
| *Glod4 isoform 2* | *Forward: 5'-ATCCTGACTCCGTTGGTGA-3'* |
| | *Reverse: 5'-TGCAGCCTTCACCATCATC-3'* |
| *Glod4 isoform 3* | *Forward: 5'-GTTCTAAACAGCCCAGATGTTC-3'* |
| | *Reverse: 5'-TTGTAGTCTCCGATGCCATAAT-3'* |
| *Actb* | *Forward: 5'-TGTTACCAACTGGGACGACA-3'* |
| | *Reverse: 5'-GGGGTGTTGAAGGTCTCAAA-3'* |
| *APP*<br>*App* | *Forward: 5'-CTTCCCCAAGATCCTGATAAACT-3'* |
| | *Reverse: 5'-CCGGGTGTCTCCAGGTACT-3'* |
| *Atg5* | *Forward: 5'-AAGGCACACCCCTGAAATGG-3'* |
| | *Reverse: 5'-TGATGTTCCAAGGAAGAGCTGAA-3'* |
| *p62* | *Forward: 5'-GGGGAAGGGTTCAATGAGAG-3'* |
| | *Reverse: 5'-AATGGGCATATTTGGGGTCT-3'* |
| *Becn1* | *Forward: 5'-GAGGAAGCTCAGTACCAG CG-3'* |
| | *Reverse: 5'-CCAGATGTGGAAGGTGGCAT-3'* |
| *Blmh* | *Forward p1: 5'-CACTGTAGCTGTACTCACAC-3'* |
| | *Reverse p2: 5'-GCGACAGAGTACCATGTAGG-3' (exon 3); Reverse p3: 5'-ATTTGTCACGTCCTGCACGACG-3' (neomycin cassette)* |
| *hAPP transgene in 5xFAD mice* | *Forward: 5'-AGAGTACCAACTTGCATGACTACG-3';* |
| | *Reverse: 5'-ATGCTGGATAACTGCCTTCTTATC-3'* |
| *hPS1 transgene in 5xFAD mice* | *Forward: 5'-GCTTTTTCCAGCTCTCATTTACTC-3'* |
| | *Reverse: 5'-AAAATTGATGGAATGCTAATTGGT-3'* |
| *mTOR* | *Forward: 5'-GCCACTCTCTGACCCAGTTC-3'* |
| | *Reverse: 5'-ATGCCAAGACACAGTAGCGG-3'* |
| *Phf8* | *Forward: 5'-TGGGAGCATGCTTCAAGG-3'* |
| | *Reverse: 5'-GATTTCAAAGCAGGGTCATCA-3'* |